A fully integrated autonomous power management system with high power capacity and novel MPPT for thermoelectric energy harvesters in IoT/wearable applications

IOP Conf. Series: Journal of Physics: Conf. Series **1052** (2018) 012127 doi:10.1088/1742-6596/1052/1/012127

A fully integrated autonomous power management system with high power capacity and novel MPPT for thermoelectric energy harvesters in IoT/wearable applications

Hamed Osouli Tabrizi[1] , H M P C Jayaweera[1] and Ali Muhtaroğlu[1,2]

[1]Sustainable Environment and Energy Systems
[2]Dept. of Electrical-Electronics Engineering
Middle East Technical University Northern Cyprus Campus
Kalkanli, Guzelyurt, Mersin 10, Turkey
Email: {hamed.tabrizi, amuhtar}@metu.edu.tr

Abstract. This paper reports a fully integrated autonomous power management system for thermoelectric energy harvesting with application in batteryless IoT/Wearable devices. The novel maximum power point tracking (MPPT) algorithm does not require open circuit voltage measurement. The proposed system delivers 0.5 mA current with 1 V regulated output based on simulations, which is the highest output current for a fully integrated converter reported in the literature for ultra-low voltage applications, to the best knowledge of the authors. Regulated 1 V output can be achieved for load range >2 kΩ, and input voltage range >140 mV. The circuit has been implemented in UMC-180nm standard CMOS technology and simulated.

1. Introduction

Elimination of the battery is desirable in emerging applications such as internet of things (IoT) and wearable healthcare devices, due to considerable miniaturization and maintenance cost benefits [1]. Recent studies have shown energy storage devices can be replaced by ambient energy harvesters [2,3]. Among various ambient energy sources, thermal energy is promising for wearable computing and similar applications, due to the availability of hundreds of microwatts of harvestable power. Despite adequate power availability, maximum open circuit voltage generated by thermoelectric generators (TEGs) exposed to the typically attainable 2-5 K temperature gradient, cannot exceed 500 mV [3,4]. Requisites of a miniaturized low-cost batteryless power management system, therefore, include 1) Full integration, 2) low start-up voltage, 3) stepped-up and regulated output voltage, and 4) relatively high output power. Charge pump converters with LC-tank oscillators have been introduced [5-8] to overcome MOSFET threshold limitations associated with low input voltage. Our group has reported solutions with an input voltage as low as 200 mV, where the maximum output power of 400 µW is achieved with a 2.7 kΩ load, which is sufficient to meet the real-time demand of most ultra-low power IoT/Wearable circuits [7,8]. Real load dynamically varies in the above-mentioned applications, as does the TEG output due to alternating ambient temperature. Thus an autonomous system is required to ensure maximum power point tracking (MPPT) under various load and source conditions.

MPPT algorithm presented in [3,9] measures TEG open circuit voltage, V_{TEG}, for impedance matching, and thus causes system disruption when disconnected. The method does not work well when the converter efficiency varies with input impedance values, as is the case for the LC-tank coupled charge pump topology. The system proposed in this paper utilizes a novel MPPT that refrains

from disconnecting the converter from source. The rest of the paper is organized as follows: The proposed system is discussed in section 2. In section 3, characteristics of the LC-tank charge pump circuit is presented. MPPT algorithm is discussed in Section 4. Section 5 presents the results, and the conclusion is provided in Section 6.

2. System Topology

2.1. TEG model and Power Efficiency

TEG first order model consists of a voltage source with open circuit voltage V_{TEG}, and a series resistance R_{TEG}, as shown connected to the power management system in figure 1. R_{TEG} restricts the maximum theoretical input power to $P_{in,max}$ as calculated from equation (1). Real input power is maximized when R_{TEG} is low and power management input impedance, Z is in the range of R_{TEG}.

$$P_{in,MAX} = \frac{(V_{TEG})^2}{4\,R_{TEG}} \tag{1}$$

Power efficiency of the system can then be calculated using equation (2) with respect to $P_{in,max}$.

$$\eta = \frac{P_{out}}{P_{in,max}} = \left(\frac{V_{out}}{V_{TEG}}\right)^2 \times \left(\frac{4\,R_{TEG}}{R_L}\right) \tag{2}$$

2.2. Power Management System

The proposed power management circuit (figure 2) is composed of an LC-tank oscillator connected to a charge pump with an adjustable number of stages, using a minimum number of PMOS switches. V_{st5} node supplies sufficient voltage to the digital MPPT even when V_{TEG} is low. Low-frequency square wave (clock) signal necessary for the MPPT block is generated using a thyristor-based ring oscillator [11] with ultra-low power consumption. The output voltage is regulated utilizing a low-dropout (LDO) regulator and a subthreshold voltage reference circuit [10]. When sufficient input power is available, op-amp and LDO start regulation.

3. LC-tank and Charge Pump Characteristics

The output voltage of the n-stage charge pump can be determined by equation (3) based on the lumped circuit model in figure 3 previously presented by our group [8]. $V_{C_{2n}}$, maximum voltage at charge pump capacitors of stage n, can be calculated in an iterative manner for n-1 stages. Input impedance of the DC-DC converter with LC-tank oscillator can be calculated using equation (4).

$$V_{out} = (V_{osc} + V_{C_{2n}})\, e^{\frac{-t}{(R_L+R_P)C}} \times \frac{R_L}{R_L + R_P}\ , t = \frac{T}{4}, \quad where \quad V_{C_{2n}} = (n-1)V_{osc} + V_{in} - \frac{t i_n}{2C} \tag{3}$$

$$Y = \frac{1}{Z} = \frac{R_M C^2\omega^2}{1 + {R_M}^2 C^2\omega^2} + \frac{(R_M + R_P)C^2\omega^2}{4 + (R_M + R_P)^2 C^2\omega^2}(n-1) + \frac{R_L C_L C\omega^2(R_M R_L C C_L\omega^2 - 1) + C\omega^2(R_L C_L + R_M C + R_L C)}{(R_M R_L C C_L\omega^2 - 1)^2 + (R_L C_L + R_M C + R_L C)^2\omega^2} \tag{4}$$

where R_P and R_M are average PMOS and NMOS average switch resistance in charge pump respectively, n is the number of stages, R_L represents load, i_n is the output current of stage n, V_{osc} is the LC-tank oscillation amplitude, V_C represents the peak voltage across the charge pump capacitors, T is the oscillation period, and V_{in} is the input voltage. Equation (3) establishes that V_{out} is directly related to n. From (4), converter input impedance has an inverse relation with n. V_{osc} also has an inverse relation with n due to the loading effect of charge pump on LC-tank.

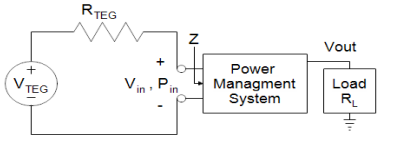

Figure 1. TEG first order model connected to the power management system.

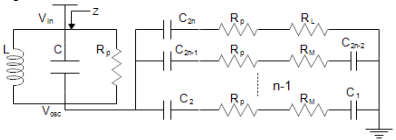

Figure 3. LC-tank and n stage charge pump circuit model proposed in [8].

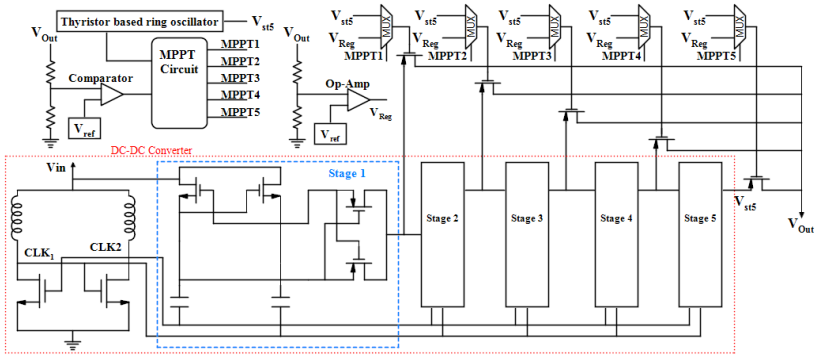

Figure 2. The proposed fully integrated power management system for thermoelectric energy harvesting.

4. MPPT Algorithm

MPPT algorithm maximizes η from equation (2) by maximizing V_{out} for a given R_{TEG}, V_{TEG}, and R_L. Therefore, regulation target is the maximum voltage that V_{out} can reach. Among the variables in equations (3), only n and C can be used to adjust V_{out}. Changing C requires an adjustable capacitor bank that significantly increases layout cost and charge redistribution losses (CRL). n is hence selected as the control parameter for MPPT. Stage 5 (last stage) is activated in the start-up state to maximize V_{out}. As long as V_{out} target is achieved, digital MPPT is inactive. When the output voltage drops below the target value, which can be a result of an increase in load or decrease in source voltage, MPPT block looks for a new optimum to reach the target voltage, by reducing the number of stages.

5. Results

R_{TEG} value varies for different products. 40 Ω is chosen in the simulations as a typical value for tiny TEGs [13]. DC-DC converter behaviour without voltage regulation is depicted in figure 4. Figure 4(a) shows that there is an optimal stage to maximize V_{out} for a given load. Loading on the LC-tank oscillator increases with the number of stages, resulting in decrease in the voltage swing as shown in figure 4(c). This also reduces input Z and V_{in} of the power management circuit, as depicted in figures 4(b) and 4(d) respectively. Therefore, output cannot be boosted up further by increasing the number of stages. Varying V_{TEG} has a similar effect as varying R_L, although this is not shown here for brevity: With fixed R_L, the optimal stage count varies with V_{TEG} value. Figure 5(a) depicts simulation results for the complete MPPT system with a given input voltage and load. Since 1 V output is not reached at start-up, MPPT block decreases the number of stages until a stage is found that delivers the target. Once target value is reached, MPPT stops. Figure 5(b) presents to a condition that leads to a lower efficiency despite increase in V_{TEG}. However, output power calculated from equation (1) is almost two times more compared to the one in figure 5(a). The power management design in this paper, which delivers maximum power to load, is practically more desirable than a design that would prioritize high efficiency over output power, as demonstrated here. Figure 6 shows the layout of the proposed system. Table 1 compares this work to the recent state-of-the art thermoelectric energy harvesting solutions in the literature. The solution in this paper provides lower cost in terms of process technology (0.18 µm), and is fully integrated. Circuit proposed in [9] is fully integrated, but use of ring oscillator has increased start-up time and limited output power. In [9], input impedance of the system is in the range of 300 Ω, which results in lower output power capacity, despite higher end to end efficiency.

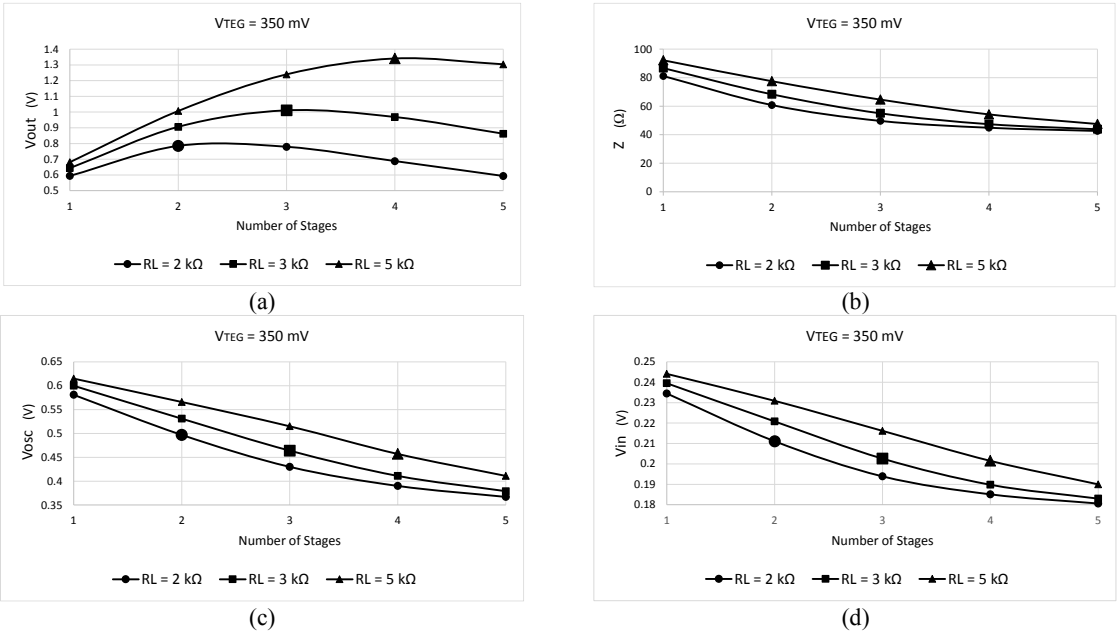

Figure 4: Optimization of charge pump stage count for each load, (a) to maximize V_{out} with fixed source voltage, and resulting change in (b) input impedance, Z, (c) LC-tank oscillation amplitude, (d) V_{in}.

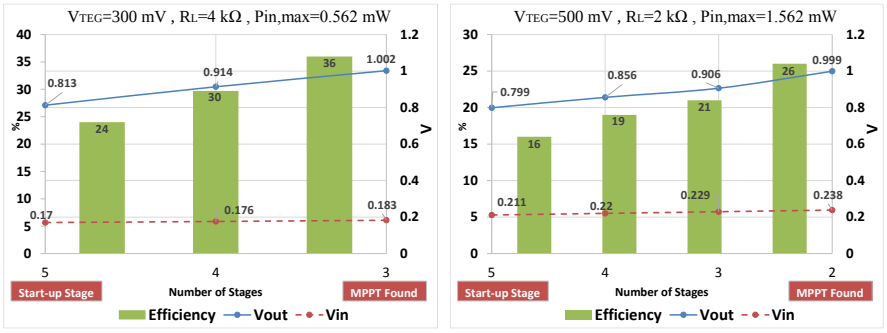

(a) (b)

Figure 5: Sample simulation results to demonstrate MPPT operation: (a) For V_{TEG}=300 mV and R_L=4 kΩ, MPPT finds optimal stage count as 3 for 1 V regulated output with 36% efficiency. (b) For V_{TEG}=500 mV and R_L=2 kΩ, MPPT find optimal stage count as 2 for 1 V regulated output with 26% efficiency.

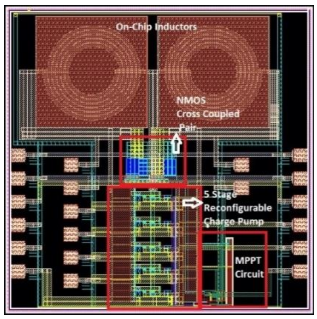

Figure 6: Chip layout: Inductors occupy 0.66 mm^2. Reconfigurable charge pump and MPPT take up 0.24 mm^2 and 0.05 mm^2 respectively.

6. Conclusion

A fully integrated autonomous power management system with high output power suitable for batteryless IoT/Wearable devices is introduced. The solution maximizes output power for a wide range of loads and input voltage variations through a novel MPPT, and delivers 0.5 mA current with 1 V regulated output at 220 mV input voltage, which is the highest output current for a fully integrated converter in the literature for ultra-low voltage applications to the best knowledge of the authors. Using this system, regulated 1 V output can be achieved for loads of > 2 kΩ and input voltage range of > 140 mV. Cold start-up from input voltages as low as 140 mV and high output power delivery are simultaneously attained in simulations due to the presence of the integrated LC-tank oscillator in the system.

Table 1. Comparison with state-of-the-art thermoelectric energy harvesters.

	[5]	[9]	[10]	[3]	[8]	This Work
Process	0.18 µm	65nm	0.18 µm	65 nm	0.18 µm	0.18 µm
Maximum Output Current	200 µA	730 µA	71 µA	358 µA	150 µA[a]	500 µA
Separate Start-Up Unit	No	Yes	No	Yes	No	No
Min V_{in} for start-up	150 mV	80 mV	350 mV	65 mV	360 mV	140 mV
Regulated V_{out}	1.8 V	0.7 V–1V	1.8V	1.8 V	1.2V	1 V
Peak End to End efficiency	N/A 73%	73%	N/A 80%	68%	43%[a]	36.7%
Off chip (L+C+R)	0+6+0	4+2+0	0+7+4	1+2+0	0+0+0	0+0+0
MPPT Tracking Time	NO MPPT	~20ms	< 180ms	< 20ms	NA	< 10ms

[a] Extracted for the V_{TEG} voltage range of < 500 mV

7. References

[1] Muhtaroğlu A 2017 *Energy Harvesting and Energy Efficiency* (Springer International Publishing) pp 63-85
[2] Balsamo D, Elboreini A, Al-Hashimi B and Merrett G 2017 Exploring ARM mbed support for transient computing in energy harvesting IoT systems. *Advances in Sensors and Interfaces (IWASI), 7th IEEE International Workshop on*
[3] Rozgić D and Marković D 2017 *IEEE Transactions on Biomedical Circuits and Systems* May 23
[4] Zoller T, Nagel C, Ehrenpfordt R and Zimmermann A 2017 *IEEE Transactions on Components, Packaging and Manufacturing Technology*. May 17
[5] Bassi G, Colalongo L, Richelli A and Kovacs-Vajna ZM 2013 *IET Power Electronics*. Jul 1 6(6) 1151-6
[6] Jayaweera HM, Pathirana WP and Muhtaroğlu A 2015 *J. of Phys: Conference Series* Vol. 660, No. 1 p 012017 IOP Publishing
[7] Jayaweera HM and Muhtaroğlu A 2016 *J. of Phys: Conference Series* Nov Vol 773, No. 1, p 012085 IOP Publishing
[8] Jayaweera HM and Muhtaroğlu A 2017 *Microelectronics Journal*. Jan 31;59:33-9
[9] Grezaud R and Willemin J 2013 *In New Circuits and Systems Conf (NEWCAS)*, Jun 16 pp 1-4
[10] Seok M, Kim G, Blaauw D and Sylvester D 2012 *IEEE Journal of Solid-State Circuits*. Oct;47(10):2534-45
[11] Mahato AK 2014 *Engineering and Computational Sciences (RAECS),* Mar 6 pp 1-5